Journal of The Electrochemical Society

The Electrochemical Society
Advancing solid state & electrochemical science & technology

OPEN ACCESS

Review—Challenges and Opportunities for Increased Current Density in Alkaline Electrolysis by Increasing the Operating Temperature

To cite this article: F. P. Lohmann-Richters *et al* 2021 *J. Electrochem. Soc.* **168** 114501

Journal of The Electrochemical Society, 2021 **168** 114501

Review—Challenges and Opportunities for Increased Current Density in Alkaline Electrolysis by Increasing the Operating Temperature

F. P. Lohmann-Richters,[1,z] S. Renz,[1,2] W. Lehnert,[1,2] M. Müller,[1] and M. Carmo[1]

[1]*Forschungszentrum Jülich GmbH, Institute of Energy and Climate Research, IEK-14: Electrochemical Process Engineering, D-52428 Jülich, Germany*
[2]*Faculty of Mechanical Engineering, RWTH Aachen, D-52056 Aachen, Germany*

The highly-efficient, low-cost, large-scale production of green hydrogen by means of electrolysis is urgently needed for achieving a decarbonized energy supply. Alkaline water electrolysis is a wellestablished technology with relatively low costs which does not require scarce noble metal catalysts, but it suffers from low current densities. Increasing the operating temperature can allow this limitation to be overcome. This article summarizes both long-standing and recent developments in alkaline water electrolysis at increased temperature and sheds light on the challenges and unique opportunities of this approach. It is found that electrochemical improvements induced by higher temperature enable competitive current densities and offer unique possibilities for thermal management. The selection and development of stable materials, catalysts, and diaphragms is challenging, but some have proven long-term stability up to at least 150 °C and promising candidates are available at up to 200 °C. Further research will allow the present challenges to be overcome by understanding and improving the basic processes and components for alkaline electrolysis at increased temperature and capitalizing on its unique advantages.
 [DOI: 10.1149/1945-7111/ac34cc]

Manuscript submitted July 31, 2021; revised manuscript received October 20, 2021. Published November 11, 2021.

Hydrogen is considered a key energy carrier in the future energy infrastructure, as it allows sector coupling and enables energy storage on a large scale. This requires highly-efficient, low-cost, large-scale hydrogen production by means of water electrolysis.

Increasing the temperature generally speeds up activated chemical reactions and therefore also improves the current density and efficiency of electrolyzers.[1–7] Depending on the particular research community, context, and time of a publication, the meaning of medium, intermediate, elevated, or high temperature varies.[1,3,6–10] In this work, we will focus on temperatures between 100 and 200 °C. As this is high with respect to conventional alkaline electrolysis, we will use the term *high-temperature alkaline electrolysis* (HT-AE), even though it is rather intermediate compared to molten hydroxide[11] or solid oxide electrolysis.

Increasing the operating temperatures in electrolyzers is not a trivial task. Elevated temperatures intensify the corrosion issues already present at low temperature under the acidic conditions in polymer electrolyte membrane (PEM) electrolyzers, and also cause membrane stability problems.[7,12–16] These challenges render PEM electrolysis unsuitable for high operating temperatures. Anion exchange membranes are a highly promising alkaline alternative to PEMs. However, one of their most important challenges is achieving sufficient long-term stability, even at temperatures below 80 °C.[17–21] Thus, to date, they cannot be considered suitable for high temperatures. So-called solid acid electrolyzers employ proton-conducting, acidic salts like CsH_2PO_4 as solid electrolyte and operate at elevated temperatures of between 200 °C and 300 °C. However, the technology is still in a very early stage of development and the inherent water solubility of the electrolytes only permits vapor electrolysis and requires delicate water management.[7,22–24]

Alkaline water electrolysis has already been demonstrated at high temperatures and is considered to have high potential for reaching current densities beyond 1 A cm^{-2} at 1.55 to 1.65 V.[7] Already in the 1970s, a strong cell voltage decrease of 0.51 V at 200 mA cm^{-2} from 80 °C to 208 °C was reported[5] and several corresponding research programs were initiated.[9] Motivated by the oil price shocks of the time period, the target application was hydrogen production using excess electricity from nuclear reactors. There were even several pilot plants that were operated at slightly elevated temperatures up to 130 °C.[9,25–28] Over the years, with PEM and solid oxide electrolysis emerging as new technologies, the interest in alkaline electrolysis diminished. Nowadays, low-temperature alkaline water electrolysis is again being intensively investigated, and recent progress has been reviewed in several publications.[29,30] Recent studies reaching impressive current densities up to 3.75 A cm^{-2} at 1.75 V and 200 °C have also renewed interest in HT-AE.[1,2,4,31] The gain in comparison to low temperature alkaline electrolysis is illustrated in Fig. 1. In conjunction with progress in other fields like material science, ceramics, and low-temperature alkaline electrolysis, these have opened up new possibilities and perspectives to reach stable, high current density and simple thermal management with HT-AE.

This review outlines the current status and future perspectives of HT-AE, covering the selection and stability of materials, catalysts, and diaphragms, as well as system design and heat and pressure control. We elaborate on the unique advantages of the technology, such as high current density and thermally-balanced operation, as well as its challenges concerning material stability, and consider promising pathways and key questions for future research in the fields of materials science, electrochemistry, and process engineering.

Electrochemical Improvements with Temperature

Thermodynamics.—The thermodynamics of water electrolysis with respect to operating pressure and temperature have been outlined in several publications and textbooks and will only be briefly recapitulated at this point.[1,4,10,31,33–3731,33–37] In an alkaline electrolyzer, water is split at the cathode into hydrogen and hydroxide ions, which then pass through the separator to the anode, where they form oxygen and water.

Total: $H_2O \rightarrow H_2 + 1/2O_2$

Cathode: $2H_2O + 2e^- \rightarrow H_2 + 2OH^-$

$$\text{Anode: } 2OH^- \rightarrow 1/2O_2 + H_2O + 2e^-$$

The reversible (minimum) voltage U_{rev} for splitting water into hydrogen and oxygen depends on the Gibbs energy ΔG:

[z]E-mail: f.lohmann-richters@fz-juelich.de

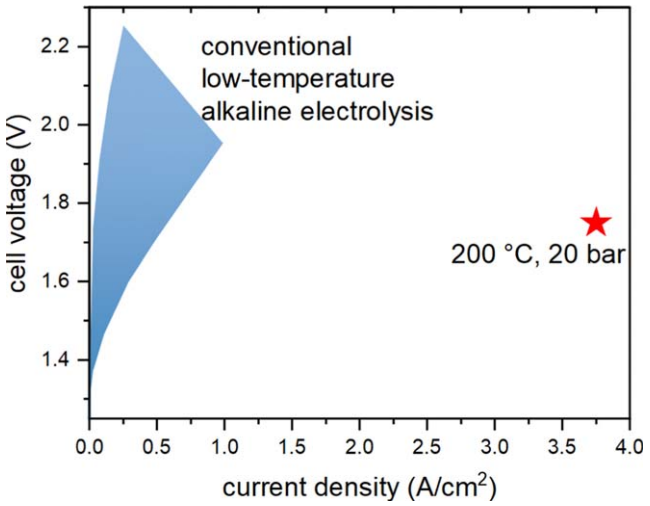

Figure 1. Illustration of the improvement of current density with high-temperature alkaline electrolysis compared to conventional alkaline electrolysis. Low-temperature range taken from Ref.,[32] high-temperature from Ref. [2].

$$U_{rev} = -\frac{\Delta G}{zF}$$

where z is the number of transferred electrons and F is Faraday's constant. The enthalpic voltage $U_{\Delta H}$ is calculated in the same way from the reaction enthalpy ΔH and includes the entropic contribution TΔS. The latter can also be supplied in the form of heat:

$$U_{\Delta H} = -\frac{\Delta H}{zF} = -\frac{\Delta G - T\Delta S}{zF}$$

The enthalpic voltage is sometimes also called thermoneutral voltage in textbooks, which can be misleading as we will point out further below. The standard values (ΔG^o and ΔH^o) can be taken from thermochemical tables,[38] as these are simply the negative of the enthalpy of formation of water at the respective conditions. In Fig. 2, it can be seen that the enthalpic voltage changes little with temperature, except for the jump from liquid water to vapor, which is due to the enthalpy of evaporation. Above 100 °C, the electrolysis of liquid water requires pressurization, and is therefore limited by the working pressures that can be reasonably attained. The reversible voltage, on the other hand, decreases with the temperature, whereas TΔS increases. The increased temperature is therefore beneficial for electrolysis, because it enables the use of thermal instead of electrical energy.

According to the Nernst equation, the voltages also depend on the pressure of the reactants. An increased pressure of the gaseous products leads to an increase of the reversible voltage. Therefore, the voltages depend on the operating pressure and the vapor pressure of the electrolyte solution, usually KOH. Balej calculated the reversible voltage for different temperatures, pressures, and concentrations, as is shown in Fig. 3.[33] As noted above, the reversible voltage decreases with the temperature, but increases with pressure. Higher electrolyte concentrations decrease the water vapor pressure and so increase U_{rev} at a given total pressure. It should be noted that although the pressure affects U_{rev}, it exerts only a minor influence on the cell voltage at significant current densities due to kinetic improvement.[26,32,39–41]

LeRoy et al. analyzed the thermodynamic limitations of water electrolysis in detail, taking additional heat-consuming processes into account.[34] Here, all energies are converted into voltages, as this allows one to directly identify which regime an electrolyzer is operating in at a given cell voltage. LeRoy et al. define the higher

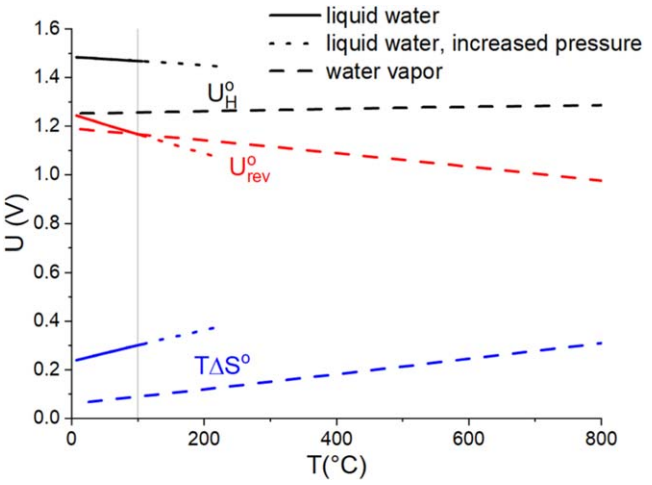

Figure 2. Standard voltages of the electrolysis of water, as calculated from JANAF tables[37]. Liquid water above 100 °C (grey line) is pressurized.

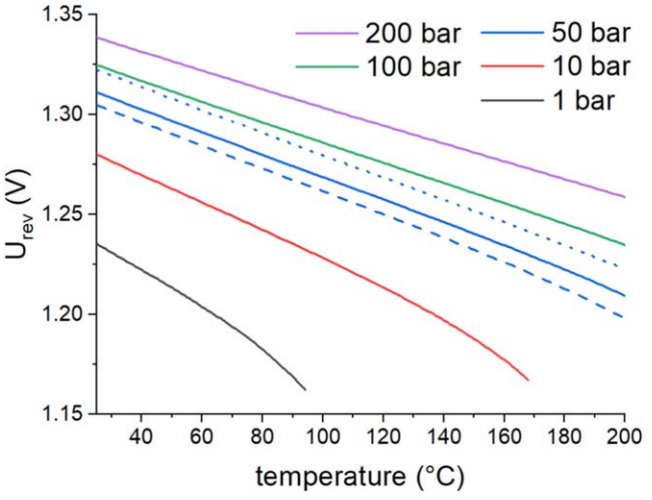

Figure 3. The reversible voltage of water electrolysis decreases with temperature, but increases with pressure and the KOH electrolyte concentration (5 wt.% dashed, 10 wt.% solid, and 45 wt.% dotted), calculated according to Balej.[33]

heating value (HHV) voltage U_{HHV} as the sum of the enthalpic voltage and U_{feed}, the voltage to heat and compress the feed water to the operating temperature and pressure. $U_{\Delta H}$ and U_{HHV} depend very little on the operating pressure and vary by only a few millivolts, even for 100 bar.[34] The addition of U_{vap}, the heat consumed by the saturation of the product gases with water vapor, yields the thermoneutral voltage U_{tn}. This contribution is especially important for high operating temperatures and depends strongly on the operating pressure. It will be discussed in more detail in the section on thermally balanced operation. It must not be confused with the enthalpic voltage, which is sometimes also called thermoneutral. Finally, we obtain the thermal-balance voltage U_{tb} by adding U_{ext}, the heat loss to the surrounding. The temperature dependence of these voltages is illustrated in Fig. 4 for 25 atm and 30 wt.% KOH.

$$U_{HHV} = U_{\Delta H} + U_{feed}$$

$$U_{tn} = U_{HHV} + U_{vap}$$

$$U_{tb} = U_{tn} + U_{ext}$$

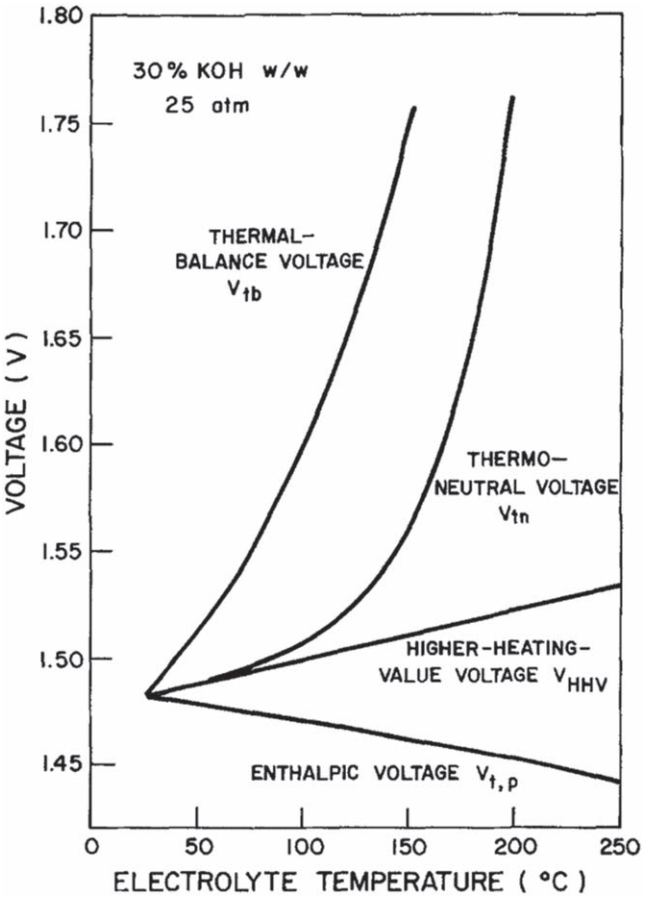

Figure 4. The voltage parameters of a water electrolyzer depend on the operating temperature. Reproduced fom Ref. 34.

The terms thermoneutral and thermal-balance voltage have not been used consistently in the literature. $U_{\Delta H}$ or U_{HHV} are sometimes referred to as thermoneutral and U_{tn} as thermo-balanced. We will utilize the terminology of LeRoy,[34] as this best reflects the practical meaning of these voltages: a perfectly isolated electrolyzer will operate at a constant temperature at the thermoneutral voltage. It will heat up or require cooling above U_{tn} and cool down or require heating below U_{tn}. An actual electrolyzer that loses heat to the environment operates in the same way with respect to the thermal-balance voltage. Note that the thermal-balance voltage depends on the actual design of the electrolyzer, whereas the thermoneutral voltage depends only on the electrolyte and the operating temperature and pressure. Both voltages can be shifted by the principal layout of the system which can enable recycling of the heat stored in the outflowing gases, e. g. by using the gases to heat the feed water.

In summary, increased temperature thermodynamically facilitates water-splitting, as electrical energy can be partially substituted by thermal energy. The heat balance is strongly pressure-dependent at increased temperatures and must be above the thermal-balance voltage if no external heat source is available. However, it will be shown in the next section that kinetic improvements with higher temperatures are more important than thermodynamic ones.

Kinetics.—The acceleration of the reaction rates with increasing temperature is common for essentially all activated chemical reactions. Increased temperatures can therefore significantly reduce the overvoltage in alkaline electrolysis. A current density of 1 A cm^{-2} at less than 1.75 V and 160 °C was considered possible in early studies.[42] In 2014, Allebrod et al. achieved 0.69 A cm^{-2} at 150 °C and 1 A cm^{-2} at 200 °C, both at 1.75 V.[31] Only two years later, this mark was improved to 3.75 A cm^{-2} at 200 °C and the same voltage.[2]

Several researchers report on the reduction of the cell voltage or overvoltage with temperature. Despite different setups and current densities, reduction rates in the cell voltage of between 3.4 and 4 mV K^{-1} between 100 °C and 200 °C were reported in several investigations.[4,5,43] Considering only the overvoltages at the electrodes, values of between 2.3 and 3.6 mV K^{-1} at 1 A cm^{-2} have been reported.[37,44,45] Interestingly, anode and cathode performance improved almost equally in these studies, although Miles observed a stronger effect in the case of the anode.[5] All of the reported improvements clearly exceed the thermodynamic decrease in the reversible voltage for liquid water (0.8 mV K^{-1}) or water vapor (0.3 mV K^{-1}) in the same temperature range. Higher temperature also requires higher pressure, to keep the electrolyte in the liquid phase. The thermodynamically expected voltage increase with increased pressure has been found to be compensated for by improved kinetics and mass transport.[26,32,39–41] However, this has apparently not been investigated for high temperature, yet.

The estimated linear voltage changes are not a very precise way of quantifying the overvoltage reduction with the temperature. A more suitable approach is to assume Arrhenius behavior and determine the activation energy of the reaction. Activation energies of between 33 and 55 kJ mol^{-1} for the cathode[45,46] and 70 to 100 kJ mol^{-1} for the anode[45,47] have been reported. For both electrodes together, an effective activation energy of 33 kJ mol^{-1} was observed.[48] It should be noted that the mechanism or at least the rate-determining step with its activation energy could depend on the investigated temperature range and the catalyst. Different catalysts will therefore improve at different rates with the temperature, potentially yielding different activity rankings as a function thereof.[7] Some researchers have suggested a change in the reaction mechanisms above 200 °C,[5,47] but this could also be due to side reactions.[4,47] The anode reaction does not exhibit typical Butler-Volmer kinetics with temperature[45] and a large surface area is not as beneficial as for the cathode.[42,45] It was suggested, that the electrocatalytic kinetics are masked by the poor conductivity of the anode's surface oxide layer.[42,45,49]

The temperature and concentration-dependence of the conductivity of KOH solutions have been investigated or tabulated in various studies,[50–55] some of which also cover temperatures beyond 100 °C.[50,52–54] The conductivity exhibits a maximum with respect to the KOH concentration, with the concentration with the highest conductivity increasing with the temperature.[51] At 30 °C, the maximum is at 30 wt.% KOH (0.69 S cm^{-1}),[51] but it is around 45 wt.% at 200 °C (2.9 S cm^{-1}).[50] The pressure-dependence of the conductivity is comparably small: From 1–500 atm, it increases by less than 2%.[52]

To summarize, high temperatures drastically improve the electrode kinetics of alkaline water-splitting as well as the conductivity of the electrolyte. With respect to the electrode kinetics, well-controlled and comparable further investigations are needed in order to better understand and quantify these gains. However, the challenge of exploiting the benefits of high temperatures lies primarily in the design and material selection for constructing an efficient and durable electrolyzer for these harsh operating conditions.

Materials for High Temperature

Corrosion stability.—The conditions in an alkaline electrolyzer at high temperature are extremely corrosive due to the temperature, the high concentration of KOH, and the presence of oxygen on the anode side and hydrogen on the cathode side. The stability of materials under alkaline conditions at high temperatures has mostly been investigated in the context of boilers, heat exchangers, and evaporators in the caustics manufacturing and paper industries.[56–62] The focus has primarily been on stainless steels and a variety of nickel alloys, which generally exhibit good corrosion resistance

under alkaline conditions. However, these conditions differ significantly from those in HT-AE, mostly concerning the presence of oxygen and hydrogen but also with respect to the temperature range, caustic type and concentration, and the voltage for current-carrying parts. Investigations under conditions relevant for HT-AE are few and far between, but yield interesting results. Two types of corrosion have been investigated thus far: Uniform or general corrosion and stress corrosion cracking (SCC). [63–65] It has been found that both are much more severe in the presence of oxygen compared to argon or hydrogen environments. The corrosion rates given in the following will therefore be those for oxygen, if not stated otherwise.

For some materials, a break-away uniform corrosion was observed, for example for alloy 600 in Fig. 5.[65] Break-away uniform corrosion means that the uniform corrosion rate is constant and relatively low for a certain time, but then dramatically increases. The time until the break-away point was mostly in the range of 2000–3000 h. Thus, corrosion tests should be performed for at least 4000 h in order to uncover potential break-away corrosion. This time scale is fairly long for laboratory tests, but well below the expected lifetime of an industrial electrolyzer. Many studies of corrosion do not cover such long time-frames, which further limits the applicability of their results to HT-AE.

Titanium and zirconium were found to completely dissolve in KOH at 220 °C.[66,67] Pure nickel, on the other hand, generally exhibits very good stability under alkaline conditions, and has been in the focus of several investigations in the context of HT-AE. No SCC was observed for pure nickel in these studies, even under oxygenated conditions.[64,65,68] Uniform corrosion rates below 10 μm a^{-1} at 200 °C and 20 bar,[64] and below 45 μm a^{-1} at 180 °C and 30 bar[68] were observed in early studies with 40 wt.% KOH. However, with a periodic renewal of the lye, a significantly increased corrosion rate of up to 800 μm a^{-1} has been reported, see Table I.[65] Gras and Spiteri argued that this could be due to fewer impurities in the solution. They observed that the presence of iron or silicate ions reduced the corrosion rate to < 5 μm a^{-1} and led to the formation of a passivation layer containing the respective ions. The incorporation of iron into the oxide layer had also been observed in one of the aforementioned previous investigations, which found 10–20 ppm Fe in the lye and low corrosion rates.[64] It could also contribute to the diverging corrosion rates in these earlier investigations, together with the differences in pressure. The conditions necessary to form the passivation layer containing iron or silicate and its long-term stability in the absence of impurities have not been clarified. Interestingly, small amounts of iron have also been found to influence the stability of anode catalysts.[69–71] Further research is needed, but if the passivation layer can be reliably created and the long-term stability confirmed, nickel could be a good choice for alkaline electrolyzers operating at high temperatures. Using a nickel coating on steel appears to be difficult at such temperatures, because any porosity must be avoided.[72]

Apart from pure nickel, several nickel-containing alloys have been tested.[65] Stainless steel AISI 310(L) has shown low uniform corrosion rates, but failed due to SCC. Alloys 400, 600, and 690 were found to be resistant to SCC, even at 180 °C. Alloy 800, which has a much lower Ni content, was susceptible to SCC at 180 °C and at 150 °C in the presence of silicates.

The uniform corrosion rates of these alloys are shown in Table I. In order to reflect the break-away phenomenon, the corrosion rates are given for the first 2000 h of the test and between 5000 and 6000 h, when they appear to have stabilized. At 150 °C, the corrosion rates of alloy 400, 690, and 800 in the first 2000 h were around 5 μm a^{-1}. Alloy 600 showed a significantly higher corrosion rate of 19 μm a^{-1}. After 5000 h, the rate decreased even further for alloy 800 but increased to 43 and 24 μm a^{-1} for alloys 400 and 690, respectively. Again, the rate of alloy 600 was significantly higher (186 μm a^{-1}). The corrosion rates of alloys 400, 690, and 800 were below 50 μm a^{-1} and they can therefore be considered resistant ($<$ 100 μm a^{-1}[159]) or category A ($<$ 50 μm a^{-1}[174]), depending on the rating system used. Only alloy 600 was fairly resistant ($<$ 1 mm a^{-1}[159]) or category B ($<$ 500 μm a^{-1}[174]).

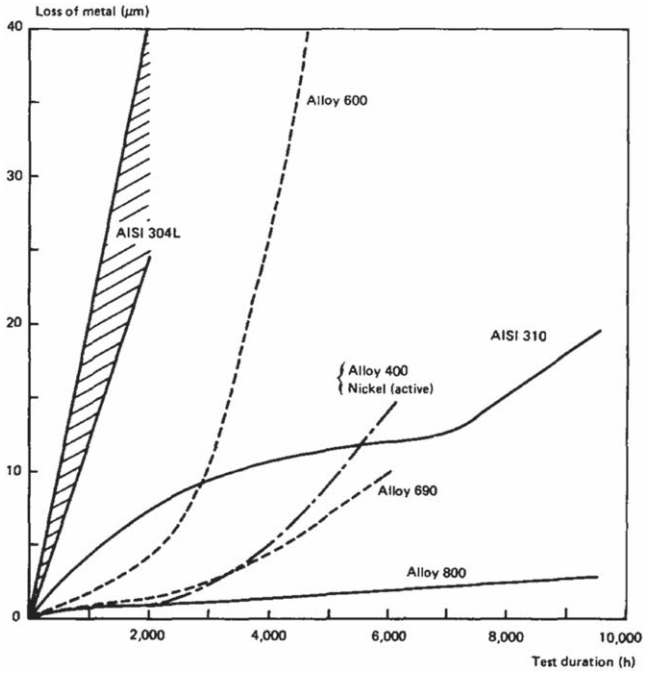

Figure 5. The general corrosion of different alloys in 38 wt.% KOH at 150 °C under oxygen shows break-away corrosion for some alloys. Reprinted from Ref. 65 with permission from Elsevier.

At 180 °C, the corrosion rates are higher than at 150 °C and alloy 600 still exhibited the highest rate of those shown here. Alloy 690 had almost four times the corrosion rate of 150 °C, but was still within the acceptable range. Meanwhile, alloy 800 exhibited increased initial corrosion but was again very stable in the long run.

Unfortunately, alloy 400 was not tested at 180 °C. The final corrosion rates of the other alloys increased by factors of between 3.1 and 3.6, from 150 °C–180 °C. Assuming an average factor of 3.4 for alloy 400, its corrosion rate at 180 °C should be around 145 μm a^{-1}. Combrade has tested alloys 400 and 690 at 200 °C, but under slightly different conditions (20 bar, 40 wt.% KOH, 2750 h).[64] Nevertheless, the observed corrosion rate of alloy 690 was similar to that reported by Gras et al. (50–140 vs 88 μm a^{-1}).[65] If the rates were indeed similar despite the shorter timescale covered by Combrade, alloy 400 could exhibit a corrosion rate of around 50–80 μm a^{-1}. Therefore, despite a lack of data on alloy 400 °C at 180 °C, the corrosion rate is probably in the range of 50–145 μm a^{-1} and can thus be considered at least fairly resistant, or category B. Additional passivation of the nickel-based alloys in the presence of iron or silicate ions has to the best of our knowledge not been investigated. However, as the alloys contain a significant amount of iron, a less pronounced effect than for pure nickel is to be expected.

Among the investigated materials, the very low uniform corrosion rate of alloy 800 stands out, but its susceptibility to SCC at 150 °C and above limits its use. Any stress in the material would have to be avoided, e.g., by stress-relief annealing. Alloy 800 l (EN 1.4558) is a low-carbon version of alloy 800 that is especially well-suited for wet chemical applications, and apparently less susceptible to SCC. It has been shown that the SCC resistance of alloy 800 under steam generator conditions depends on the quantities of C, Al, and Ti therein, as well as on the thermal treatment.[58,75] The low nickel content and high mechanical strength of alloy 800 or 800 l compared to pure or alloyed nickel would make its use economically attractive. Thus, alloy 800 l could indeed be a good choice for HT-AE conditions, even though further investigations are needed to confirm this. Other common nickel alloys such as Hastalloy C-276, and alloys K-500, 625, and 825 generally exhibit good stability under

Table I. Uniform corrosion rates[65] and composition[73] of selected alloys in 38 wt.% KOH under 40 bar O_2.

T (°C)	Alloy		Corrosion rate (μm/a)	
	Name	Approx. composition	0–2000 h	5000–6000 h
150	400	67Ni-31.5Cu-1.2Fe	4	43
	600	76Ni-15.5Cr-8Fe	19	186[a)]
	690	58Ni-29Cr-9Fe	6	24
	800	33Ni-21Cr-40Fe-0.8(Al + Ti)	4	2[b)]
	Nickel		4	50
180	600	76Ni-15.5Cr-8Fe	44	588[a)]
	690	58Ni-29Cr-9Fe	17	88
	800	33Ni-21Cr-40Fe-0.8(Al + Ti)	96	7[b)]
	Nickel		500–800	500–800
	Nickel	In presence of Fe or Si[c)]	< 5	< 5

a) 4000–5000 h. b) susceptible to stress corrosion cracking. c) Fe in the range of a few mg l^{-1}, Si 0.1–3.2 g l^{-1}.

alkaline conditions, even at elevated temperatures,[57,62] and other highly stable alloys like alloy 59 have been developed in the meantime. However, their stability under HT-AE conditions must still be investigated.

Based on the limited available literature, we can conclude that passivated pure nickel (or a coating thereof) and SCC-resistant alloy 800 l appear to be the most promising materials for HT-AE up to 200 °C, but that the passivation and SCC resistances are fully tested and understood. For temperatures up to 150 °C, several materials, such as alloys 400, 690, and 800, appear to be suitable. Alloys 400 and 690 exhibit corrosion rates that can be acceptable for use in experimental setups at up to 180 °C, especially if these are not continually operated at the maximum temperature and frequently inspected. Considering its fairly widespread use, components made from alloy 400 are more easily available than those from alloy 690. Thus, alloy 400 could be the best choice for laboratory setups to investigate HT-AE if appropriate corrosion monitoring is assured.

It should not be overlooked that early projects aimed at operation at 200 °C were abandoned due to material problems.[43,72] Identifying or developing stable materials for use in such harsh conditions is a challenge. However, at somewhat lower temperatures, e.g., below 150 °C, the range of promising materials substantially increases, as is outlined above. Moreover, the uniform corrosion rates of the materials further increase at the water line, in crevices and at welded joints. This has been observed for nickel,[64,68] but detailed testing for the other alloys is still necessary. These areas with enhanced corrosion can be minimized in the design of HT alkaline electrolyzers, but not completely avoided. A protective coating, for example with perfluoroalkoxy alkanes (PFA) or polytetrafluoroethylene (PTFE),[59] might reduce the risk. Protective oxide coatings have also been suggested[7] and aluminized steel has been used for electrolysis using molten hydroxides.[11] For stack materials that are subject to electric potentials, the corrosion at the relevant potentials must be investigated, in addition to free corrosion. In any case, in light of the limited data, close monitoring is necessary to maintain safe conditions.

Catalysts.—Catalysts are needed in water electrolysis to reduce electrode overvoltages and have a direct impact on the electrical efficiency. Therefore, even for a mature technology such as low-

Table II. Overview on stability of catalysts tested in high-temperature alkaline electrolysis. T: temperature, t: test duration.

	Material	T	KOH	conditions	t	degradation
Anode	RuO_2[45]	>100 °C	50 wt.%	0.1–1 A cm^{-2}	few h	dissolves
	Raney Ni [84]	100 °C	40 wt.%	0–0.4 A cm^{-2}	7200 h	slow
	[85]	160 °C	—	—	—	unstable
	[86]	200 °C	35 wt.%	1 A cm^{-2}	100 h	unstable
	porous Co[87]	90 °C–130 °C	30–40 wt.%	—	—	fast
	porous $NiCo_2$[87]	90 °C–130 °C	30–40 wt.%	1 A cm^{-2}, η < 270 mV	3000 h	stable
	Co_3O_4/Ni[88]	120 °C	40 wt.% NaOH	1 A cm^{-2}	10,000 h	slow
	Co-oxide[31]	200 °C	45 wt.%	1.5 V	24 h	stable
	[31]	250 °C	45 wt.%	1.5 V	100 h	unstable
	La–Ni(−Fe)-perovskites[89]	100 °C	31, 45 wt.%	ex situ	168 h	stable
	[89]	220 °C	31, 45 wt.%	ex situ	168 h	unstable
	Co–(Ni–Fe) ox. synth. in situ[87,90]	90 °C–130 °C	30–40 wt.%	1 A cm^{-2}	> 400 h	unstable
	$La_{0.5}Sr_{0.5}CoO_3$/porous Ni[44]	160 °C	40 wt.%	1 A cm^{-2}	2800 h	stable
	Ag-nanowires/NiFeCrAl foam[2]	200 °C	45 wt.%	0.5 A cm^{-2}	400 h	stable
	Ni–Fe–Hydroxides				not tested at HT	
Cathode	Raney Ni[85]	190 °C	40 wt.%	ex situ		unstable
	[46]	200 °C	NaOH	intermittent pol.		unstable
	[86]	200 °C	35 wt.%	1 A cm^{-2}	100 h	stable
	Ni-sulfide[6,46,91]	<110 °C	—	—	—	unstable
	Ti-/Mo-doped porous Ni[44,85]	160 °C	40 wt.%	1 A cm^{-2}	8000 h	stable
	Raney NiCo[6]	—	—	—	—	stable
	inconel foam[2]	200 °C	45 wt.%	0.5 A cm^{-2}	400 h	stable
	Ru-film/Ni[90]	120 °C	40 wt.%	1 A cm^{-2}	600 h	stable

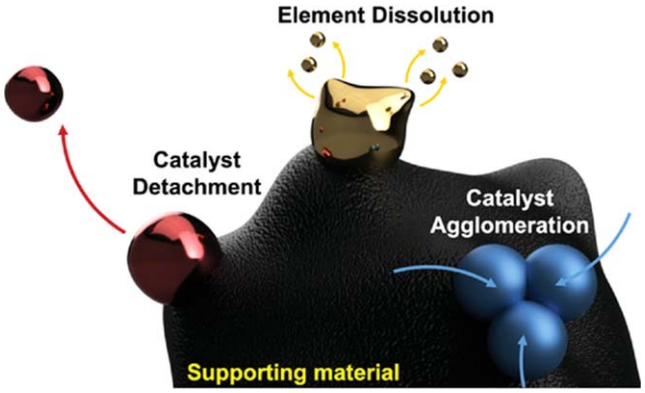

Figure 6. Illustration of degradation mechanisms of water electrolysis catalysts. Reproduced with permission from Ref. 77, © 2020 Wiley-VCH GmbH.

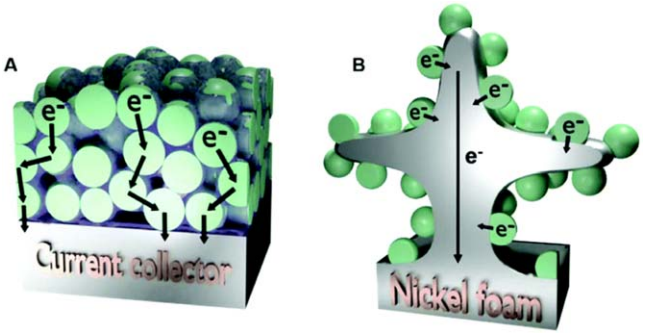

Figure 7. Catalysts directly grown or deposited on metal foam offer improved stability due to a good connection to the substrate. Reproduced from Ref. 80 with permission from the Royal Society of Chemistry.

temperature alkaline electrolysis, the catalysts remain an intensely-investigated component, and have been duly revisited in several recent reviews.[18,76–79] Much of the progress on catalysts for low-temperature alkaline electrolysis is probably transferable to HT-AE technology. The benefit of elevated temperature depends on the activation energy of the reaction and therefore on the catalyst. This could even lead to a change in the ranking of catalysts depending on the operating temperature.[7] Therefore, comparable temperature-dependent measurements of the catalyst performance are needed to identify the best candidates. Such data is not available to date.

Most catalysts fail due to insufficient stability in the harsh conditions of HT-AE which is probably one of the reasons for a lack of catalyst data under these conditions. We will therefore focus on the stability. The catalysts investigated under HT-AE-conditions are summarized in Table II. Even at low temperatures, catalyst stability is often neglected or insufficiently investigated, with much smaller time scales and current densities than would be needed for industrial use.[76,77] According to Jin, degradation is mostly due to catalyst agglomeration, dissolution and detachment, illustrated in Fig. 6.[77] Dissolution depends on the catalyst material itself, its solubility, and the formation of protective passivation layers, often involving dopants. In order to avoid agglomeration and detachment, a stable connection between the support and catalyst is essential. In particular, stable electrodes can be achieved with catalysts directly grown or deposited on a conductive substrate such as metal foam, illustrated in Fig. 7.[76,77,80] Such a stable connection between the catalyst and conductive support is especially important for HT-AE. Growing oxide layers, especially at the anode, can cause insufficient electrical contact or even isolate the catalyst particles, rendering them inactive.[49,77,81–83] Growing a thin, electrically (semi)conducting, stable, and active protective layer would be ideal. However, such an ideal layer has not yet been achieved to the best of our knowledge, especially at elevated temperatures. Clearly, the support itself must be chemically stable as well. Nickel foam, which is often used as support in low-temperature alkaline electrolysis, has only been observed to be a stable anode support when coated with a NiFeCrAl alloy.[2]

Anode.—Despite the limited number of publications on HT-AE, several studies cover the anode stability. RuO_2 has been found to dissolve rapidly,[45] which is in accordance with the dissolution observed at low temperatures.[77]

Highly porous nickel anodes exhibited fairly slow degradation over 7200 h at 100 °C,[3,84] but were reported to be unstable due to excessive oxidation at >160 °C.[85,86] The same porous nickel with a coating of $La_{0.5}Sr_{0.5}CoO_3$ perovskite was found to be stable at 160 °C and 1 A cm^{-2} over several thousand hours.[44] However, additives and sufficient sintering is needed to ensure the formation of a single phase instead of separate oxides, and continuous anodic polarization is also required for stable operation.[8,87] Similar perovskites are also investigated for use at low temperatures,[77,78,92,93] but data on stability and high temperatures is scarce. Adolphsen et al. exposed various La-Ni(-Fe)-perovskites to 31 and 45 wt.% KOH at 100 and 220 °C, respectively, but none was stable at 220 °C.[89] It has been suggested, that several mixed oxides of cobalt or nickel are not actually stable but form a similar surface layer after initial leaching, resulting in similar activity which is almost independent of the initial composition.[49]

Porous cobalt was found to dissolve quickly,[87] and in situ formed cobalt oxides containing nickel and/or iron were also not stable at 130 °C.[87,90] $NiCo_2$ and Co_3O_4/Ni were found to be stable under certain conditions at 130 and 120 °C, respectively.[87,88] Allebrod et al. successfully employed cobalt oxide as a catalyst at 200 °C over 24 h, but observed degradation at 250 °C.[31] With Ag-nanowires as a catalyst, at 200 °C they reported stability over several hundred hours if a chemically-stable NiFeCrAl-coated foam was used as a support.[1,2] This underlines that not only the catalyst itself needs to be stable. Ganley performed HT-AE tests using lithiated or cobalt-plated nickel, [4] which are also used in molten carbonate fuel cells operating under very harsh conditions.[94] Despite testing up to 400 °C, the stability was not investigated due to technical limitations.

Cathode.—The hydrogen evolution reaction in alkaline conditions is much slower than in acids.[95] and causes an overpotential of similar magnitude as the oxygen evolution reaction.[96] High-performance cathode catalysts are therefore a key element in alkaline electrolysis, as opposed to acidic electrolysis. Nickel with a very high surface area is frequently used to reduce the overvoltage of the cathode. It is usually obtained by means of galvanic deposition, plasma-spraying, or galvanization, yielding a nickel alloy such as Ni–Al or Ni–Zn, from which Al or Zn is subsequently leached, resulting in a highly porous structure, usually referred to as Raney nickel. [44,97–99] High-surface-area nickel cathodes degrade at high temperatures[6,44,46,86] but are stable if continually polarized.[86] Maintaining a minimum cell potential to avoid degradation of the electrodes is also known from low-temperature alkaline electrolysis. The addition of other elements to Raney Ni, especially Ti and Mo, yielded a catalyst that was stable over 8000 h at 160 °C.[44] Co and Fe have also been found to improve cathode performance at high temperatures.[6,45] However, catalysts with a much lower surface area were also employed at high temperatures: a dense ruthenium film on nickel was used as a cathode at 120 °C[90] and inconel foam at 200 °C.[2]

Future catalysts.—From the above, it is apparent that promising catalysts for HT-AE are available, despite the harsh conditions they must endure: For the anode, several cobalt oxides, with $La_{0.5}Sr_{0.5}CoO_3$ having been tested most intensively, and silver nanowires on a stable alloy foam showed good performance and stability. For the cathode, Mo-doped Raney nickel has shown stability over several thousand hours. However, the number of

studies on catalysts for HT-AE is still very limited, and further research is needed especially on the anode, as this is probably the most challenging component in terms of stability.

Nevertheless, it is worth considering catalysts that have proven stable and effective under different conditions, like molten carbonate fuel cells or solid oxide electrolyzers. Testing established and extremely stable catalysts used in low-temperature alkaline electrolysis is an obvious step, but the lack of data on long-term stability[76,77] renders the selection difficult. Mixed oxides or hydroxides of nickel and iron have proven to be both stable and highly active at low temperature,[69–71,76–78,100–102] but have apparently not been tested for HT-AE. The role of the different elements in the oxygen evolution reaction remains under debate,[78,101,103–105] As is discussed in the section on corrosion stability, nickel is stabilized under HT-AE anode conditions by traces of iron, which are incorporated into the surface oxide layer. Ni-Fe oxides and hydroxides are therefore promising candidates as anode catalysts for HT-AE. They can also be directly grown on high-surface-area metal supports. [100,106,107] Corrosion engineering is another promising approach for the synthesis of stable supported catalyst.[108]

The stability of the cathode at high temperature is less of an issue than of the anode. Therefore, it is promising to employ new or established cathode catalysts from low-temperature alkaline electrolysis, such as structured transition metal alloys, oxides, chalcogenides, phosphides, carbides and nitrides.[76,78] Metal carbides could be a promising candidate, as these appear to be stable even under acidic conditions at high temperatures[23] and have also received increasing attention for alkaline electrolysis applications.[78] A project on electrolysis using molten hydroxides at 550 °C did, unfortunately, not state any details on the catalysts employed.[11]

For the catalysts which are found to be stable and suitable for HT-AE, more detailed investigation on the temperature-dependent performance, electrode fabrication and structure, stability criteria, and structure-property relationships are needed to provide basic understanding for future design and optimization. For in-depth understanding of the activity and stability of the catalysts, operando studies would be very valuable,[109] but difficult to perform given the harsh conditions.

Polymers.—High temperature and strongly alkaline conditions are also highly challenging for parts made from or coated with polymers. Polymers are usually needed as seals or gaskets for connections and valves, and as protective coatings for other components. They are also considered a structural material for alkaline electrolysis at lower temperatures.[110] The stability of various polymers under HT-AE conditions has been investigated and is summarized in Table III. Polybenzimidazole, which is well-known from high-temperature fuel cells, is not stable under strongly alkaline conditions, even at 80 °C.[111,112] Polyethersulfone and polyarylsulfone were found to only be stable up to 100 °C in KOH solution, whereas polyarylethersulfone has been found to be stable at up to ca. 120 °C.[8,112] Fluorinated ethylene propylene, perfluoroalkoxy alkane (PFA), polytetrafluoroethylene (PTFE), and Polyphenylene sulfide, however, have been found to be stable in concentrated KOH at up to 120 °C, 200 °C, 220 °C, and 230 °C, respectively.[8] The tested polyphenylene sulfide (Ryton R6) seems to no longer be available and the varieties available today have not yet been tested. Thus, only PTFE and PFA are easily available and suitable for high temperatures in contact with KOH. Where pure materials cannot be used, PFA or PTFE with fillers could be applicable. These fillers must also be stable, which excludes some common types, such as glass fibers. Most of the common elastomers used for O-rings have never been tested under HT-AE conditions, and already fail at lower temperatures or KOH concentrations.[59] The materials that resist the temperature but not the alkaline conditions could be used with a PFA or PTFE coating. Therefore, despite the extremely demanding conditions, several polymers are available for use in HT-AE.

Diaphragms and membranes.—The membrane or electrolyte-filled diaphragm is at the core of any electrolyzer or fuel cell, and decisive for several of its properties, such as the operating temperature. This is also reflected in the usual categorization of these devices on the basis of their electrolyte, e.g., alkaline, polymer electrolyte membrane, or solid oxide electrolyzer.

In alkaline electrolyzers, porous diaphragms are usually employed. HT-AE exceeds the maximum operating temperature of common low-temperature diaphragms such as Zirfon (up to 110 °C–120 °C), which is based on polysulfone and ZrO_2, as the employed polymers are not sufficiently stable.[113–115] A diaphragm must generally be mechanically and chemically stable, separate the product gases, and provide high ionic conductivity. The latter depends on thickness, good wetting of the diaphragm by the liquid electrolyte, and high porosity, but the pores should be small enough to avoid the formation of bubbles in them.[8,116,117]

H_2 and O_2 crossover must be avoided in order to ensure the safe operation and high purity of the product gases. The maximum cross-flow of gases dissolved in the electrolyte can be estimated based on the hydrodynamic permeability of the diaphragm and the diffusion of the dissolved gases.[8,66,67,117,118] Pores below 100 nm were suggested to achieve a high gas purity.[116] Although the gas solubility decreases with temperature for low concentrations and temperatures, it increases with temperature at high KOH concentrations and temperatures.[48,53,118,119] Abe et al. observed increasing hydrogen crossover with 30 wt.% KOH between 70 °C and 120 °C, although the insufficient stability of the diaphragm could also have influenced the measurement.[39] Therefore, a detailed analysis of hydrogen crossover is needed for any promising diaphragm or membrane for the respective operating conditions. However, crossover by mixing the electrolyte streams from the anode and cathode is usually more important than crossover through the diaphragm, and can be mitigated by intermittent or partial mixing.[39,119,120]

Although the basic challenges of conductivity and crossover are essentially the same in HT-AE as in low-temperature alkaline electrolysis, the crucial difference is the choice of a material that can withstand the aggressive conditions. Promising materials are summarized in Table IV. Asbestos has long been used as a diaphragm in alkaline electrolysis. This material has been abolished due to its cancerogenicity, but it was also shown to be unstable at temperatures above 100 °C, and is therefore not suitable for

Table III. Polymers for use in alkaline electrolysis at high temperature.

Polymer	Max. temperature for use in contact with conc. KOH	Processable from solution
Polybenzimidazole[111,112]	<80 °C	yes
Polyethersulfone[8,112]	100 °C	yes
Polyarylsulfone[8,112]	100 °C	yes
Polyarylethersulfone[8,112]	120 °C	yes
Fluorinated ethylene propylene[8]	120 °C	no
Perfluoroalkoxy alkane[8]	200 °C	no
Polytetrafluoroethylene[8]	220 °C	no
Polyphenylene sulfide[8]	230 °C	no

Table IV. Diaphragm materials for high-temperature alkaline electrolysis. T: tested temperature, R: ionic resistance, t: test duration.

	Material	T	R (mΩ cm^2)	Thickness	t	Stability
	Ni[9,86,112]		*electrically conductive*			instable
Porous oxides	NiO[3,81,84,121]	120 °C	ca.70 @25 °C	400 μm	6000 h	stable
	$BaTiO_3$[9,66,67,117]	160 °C	150 @25 °C	400 μm	2500 h	stable
	stab. ZrO_2[2]	200 °C	58 @200 °C	180 μm	400 h	stable
	$SrTiO_3$[1,31]	250 °C	230 @150 °C	1300 μm	100 h	stable
	$SrZrO_3$[11]	550 °C	*molten hydroxide electrolysis*			
	$LiAlO_2$[94]	650 °C	*molten carbonate fuel cells*			
Polymers	radiation grafted PTFE[9,112,122,123]	120 °C				instable
Composites	Polyantimonic acid-PSU[25,88,124]	120 °C	120 @120 °C	350 μm	4000 h	stable
	Polyantimonic acid-PTFE[112,124]	>120 °C	*scalability problems*			
	PTFE + various oxides[39,112,125]	>120 °C				instable
	PTFE-ZrO_2[9,124]	160 °C	240 @160 °C	—	3600 h	stable
	Layered double hydroxides[126,127]	146 °C	*electrolysis in neutral conditions*			

HT-AE.[9,112] Sintered porous nickel has been tested as an alternative diaphragm but also found to be unstable in the long run.[9,86,112] In addition, the electric conductivity of metallic nickel makes a 0-gap configuration impossible, which impedes low cell resistances being reached.

Porous oxides.—Porous oxide diaphragms avoid the problem of electric conductivity. Divisek et al. prepared NiO diaphragms via the thermal oxidation of porous nickel.[3,81] These have an operating temperature range of 100 °C–120 °C and were shown to be stable for 6000 h.[84,121] At higher temperatures and hydrogen pressures, NiO was found to be reduced to metallic nickel.[121] Thermodynamically-speaking, any oxide containing a metal that is more noble than hydrogen is prone to reduction during electrolysis.[66,87] NiO diaphragms are therefore limited to relatively low temperatures in order to avoid reduction, which would render them electrically-conductive. In addition, the adsorption of oxygen turns NiO into a semiconductor.[84]

Titanates are also a potential material for use in oxidic diaphragms.[66,112,117] Again, Ni-titanates can be reduced by hydrogen,[9] but the titanates of metals less noble than hydrogen are stable, such as $CaTiO_3$.[9,66,67,117] The $CaTiO_3$ diaphragms were sintered onto a nickel net as support for mechanical stability and flexibility.[42,66,117] With a thickness of 400 μm, these exhibited specific resistances down to 150 mΩ cm^2 (25 °C, 30 wt.% KOH) and were tested up to 160 °C for 2500 h without any deterioration. The pores of the diaphragm are fairly large (several μm) and therefore not optimal for avoiding hydrogen crossover.

More importantly, the thickness of the supporting nickel net limits how thin a diaphragm can be made. Although oxides require a stable support,[112] they can also be supported by the electrodes, which enables a lower thickness; see Fig. 8. [1,2,117] The support material also limits the sintering temperature, as it must not melt. With nickel as a support (the melting point of which is 1455 °C) and a sintering temperature of at least two thirds of the oxide melting temperature, this excludes various promising zirconium-based oxides.[117] However, lower sintering temperatures can be employed if a high density is not required, such as for porous structures.[128] Therefore, previously discarded materials, such as zirconates, are still promising candidates. In addition, techniques that keep the substrate at low temperatures and do not require additional sintering, such as plasma-spraying, can be used.[112,129]

Allebrodt et al. developed metal-foam-supported $SrTiO_3$ diaphragms with sintering at a temperature of only 1000 °C (about half of the melting temperature).[1,31] Despite a relatively high thickness of 1300 μm, a remarkable resistance of around 230 mΩ cm^2 was observed at 150 °C with a 45 wt.% KOH. Using tape-casted yttria-stabilized zirconia and sintering at the same temperature, the thickness was reduced to 180 μm, which yielded down to 58 mΩ cm^2 at 200 °C.[2] Although the performance of the cells significantly differed, stable operation was observed beyond 400 h. In contrast to earlier work by Wendt et al., these diaphragms have pore sizes in the sub-micrometer range, which is beneficial for gas purity. $SrZrO_3$ was found to be highly stable in electrolysis with molten hydroxides of up to 550 °C[11] and could therefore also be a promising material for HT-AE diaphragms. Similarly, materials established from molten carbonate fuel cells, such as $LiAlO_2$ could be worth testing.[94]

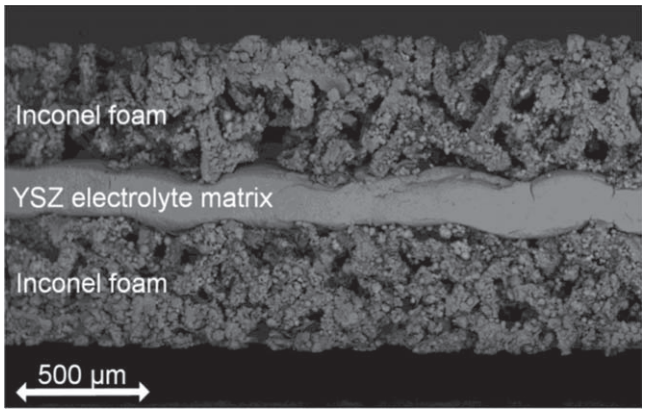

Figure 8. A metal support allows to employ very thin ceramic diaphragms of only 180 μm thickness. Reproduced from Ref. 2 licensed under CC BY 4.0.

Further improvements can be expected by applying new approaches for the preparation of thin, porous ceramic layers from different fields, which have recently been reviewed.[128–130] These advances primarily originate in the fields of solid oxide fuel cells, filtration, and thermal barrier coatings, and enable, for instance, free standing films with thicknesses of only 3 μm,[131] and supported layers with 260 nm thicknesses and pore sizes of around 3 nm.[132] Transfer of the employed technologies to diaphragms for HT-AE should enable significant further reductions in thickness, as well as the optimization of the pore structure, improving the ionic conductivity and gas cross-over.

Polymers and composites.—All of the polymers that are stable under HT-AE conditions (see above) are hydrophobic, and thus not suitable as diaphragm materials in their pure form. They must be hydrophilized in order to achieve high conductivity and stable operation. PTFE has been hydrophilized by means of grafting, e.g., with acrylic acid groups.[9,112,122,123] Unfortunately, this modification is not stable under HT-AE conditions and the diaphragms become hydrophobic over time. Organic–inorganic composites can overcome this limitation. The polymer provides mechanical stability and flexibility, whereas the stable inorganic oxide provides a

hydrophilic surface. Despite a range of possible polymers and oxides being used, the preparation of such composite diaphragms is not a trivial task.[112]

Polysulfone (PSU) has been used as a polymeric binder in several studies. Its solubility in various organic solvents enables the solution casting of diaphragms. Composite diaphragms of PSU with MgO have been prepared that exhibit an ionic resistance of 180 mΩ cm^2.[125] Diaphragms of polyantimonic acid with PSU have been quite extensively explored. These require NaOH as an electrolyte for reasons of stability, but still showed resistances down to 120 mΩ cm^2 at 120 °C with a thickness down to 350 μm.[25,88,124] The conductivity depended strongly on the hydrophilicity of the diaphragm and decreased sharply with low contents of polyantimonic acid. The operating temperature of these diaphragms was limited to around 120 °C due to the instability of PSU in alkaline solutions at higher temperatures.[112,124] This also limits the temperature range of the presently used Zirfon diaphragms. PSU-based diaphragms are therefore only suitable for electrolysis at slightly elevated temperatures.

PTFE enables significantly higher temperatures. Composites of polyantimonic acid with PTFE were discontinued due to scalability problems with the employed cold rolling technique.[112,124] The direct formation of potassium titanate on a porous PTFE sheet yielded better ionic resistance (280 mΩ cm^2 at 25 °C in 30 wt.% KOH) than the impregnation of PTFE with potassium titanate.[112] However, electrolysis tests of up to 120 °C revealed that the diaphragm was not stable, but lost its hydrophilicity.[39] Diaphragms made of PTFE and $Mg(OH)_2$ or $Zr(OH)_4$ were tested at up to 160 °C, but showed fairly unstable resistances above 600 mΩ cm^2 in 40 wt.% KOH.[125] Early composites of PTFE with several oxides were found to be inferior to asbestos separators,[112] whereas a composite of PTFE with ZrO_2 was found to be chemically-stable in KOH at 160 °C.[124] Its specific resistance improved with decreasing particle size[124] and reached about 200 mΩ cm^2 at the same temperature.[9]

PFA and polyphenylene sulfide could be used instead of PTFE, as they are also stable at high temperatures (see section on polymers), but there seem to be no reports on such composites. However, these polymers cannot be casted from solutions, which impedes the application of the processing technology obtained from well-developed low-temperature diaphragm preparation. However, new processing approaches could enable high performance diaphragms for high temperatures to be achieved. PFA or polyphenylene sulfide would, for instance, allow the melt mixing of composites.[133]

Future diaphragms.—Presently, porous oxides are the most promising material for stable diaphragms for HT-AE. Their stability is well understood and has been demonstrated. With recent developments in ceramic technology, it should be possible to prepare supported, thin, and highly porous oxide membranes with small pore sizes. In the medium term, the conductivity must become comparable to the current state-of-the-art in low-temperature diaphragms, e.g., of Zirfon (100–70 mΩ cm^2 at 80 °C, 30 wt.% KOH),[115,134] or even acidic polymer electrolyte membranes (e.g., Nafion 212 with 34 mΩ cm^2 at 80 °C).[135] Pore sizes below 100 nm would be beneficial for high gas purity.[116,136] Both high conductivity and small pore sizes have already been achieved recently,[2,31] which should serve as a starting point for further investigations of materials, long-term stability, preparation techniques, and electrochemical properties.

Although no stable hydrophilic polymer seems to be available, polymer inorganic composites could be suitable as diaphragms at high temperatures. For temperatures above 120 °C, new preparation routes are needed to prepare high-performing diaphragms with stable polymers. PTFE with ZrO_2 has shown promising performance but it will be crucial to ensure permanent hydrophilicity of the composite diaphragms.

In terms of cross-over, a non-porous membrane could be superior to a porous diaphragm and also enable differential pressure operation, as is common in PEM electrolysis. It could also enable operation at lower KOH concentrations, easing the corrosive conditions. High temperatures appear to be inaccessible using current anion exchange membrane materials due to the stability issues, even at lower temperatures.[17–20] However, composite membranes with inorganic hydroxide-conducting materials with stable polymers could offer an alternative approach. Layered double hydroxides are conductive and applicable in water electrolysis, even at high temperatures.[126,127] The key challenge is to prepare such a composite membrane that features both sufficient conductivity and mechanical stability.

System-Level Improvements with Temperature

Apart from the increased electrical efficiency, an HT-AE system could offer new opportunities in terms of system design. Most straightforward is the exploitation of waste heat. As the operating temperature is significantly higher than in low-temperature electrolyzers, the surplus heat is more valuable for waste heat utilization because of its higher exergy content.[137] In cases where no benefit can be derived from the waste heat, the cooling of the system against its surroundings is significantly simplified due to the higher temperature difference. In addition, the increased temperature enables vapor or liquid feed and thermally balanced operation.

Feed composition.—An HT-AE can be fed with steam or with liquid lye. An indirect vapor feed and a lye feed only to the cathode have also been suggested but were apparently not widely adopted.[138,139] Allebrod et al. employed a steam feed for the investigation of an HT-AE between 150 and 250 °C.[1,2,31] The system allowed detailed control of the operating conditions and avoided the corrosion issues associated with the circulation of lye at these temperatures. In addition, the required voltage is lower and a reversible electrolyzer fuel cell can be more easily realized if steam is employed.[7] Steam electrolysis is especially attractive if heat for steam production is readily available. If this is not the case, balancing the heat flux becomes especially challenging. However, a steam feed for HT-AE with an immobilized liquid electrolyte has the fundamental disadvantage that the partial pressure of water must be exactly at the vapor pressure of the immobilized electrolyte throughout the entire stack. If the partial pressure is too high, the electrolyte is diluted or even becomes washed out; if it is too low, the electrolyte dries out. In both cases the active area in the electrodes will change. This requires precise control of the water partial pressure,[140] especially during startup and shutdown. Even more importantly, this limits the conversion of the water, as the partial pressure at the inlet and outlet must not significantly deviate. These limitations can be mitigated by an appropriate stack and system design, but this might be challenging. In addition, it has been observed that supplying vapor instead of liquid water can lead to transport limitation at increased current densities.[141,142] Given these limitations, a feed of liquid lye to the HT-AE appears to be much more practical from a system design point of view, and will be discussed in more detail in the following. However, it should be noted that these limitations do not apply when a dense, solid electrolyte is used. In this case, a steam feed might be a viable option and could reduce corrosion issues.

Thermally balanced operation.—The heat balance of electrolyzers has been addressed in several studies.[34,37,41,43,143] In any electrolyzer, the overvoltages at significant current densities result in the generation of heat. On the other hand, heat is consumed, for instance by the evaporation of water into the product gases, by means of heating the feed water, and also by dissipation into the surroundings of the electrolyzer. The evaporation of water from the electrolyte into the product gases is one of the most important heat sinks in an electrolyzer. The equilibrium partial pressure of water in the product gases is equal to the vapor pressure of the electrolyte at the respective temperature and concentration. The heat of

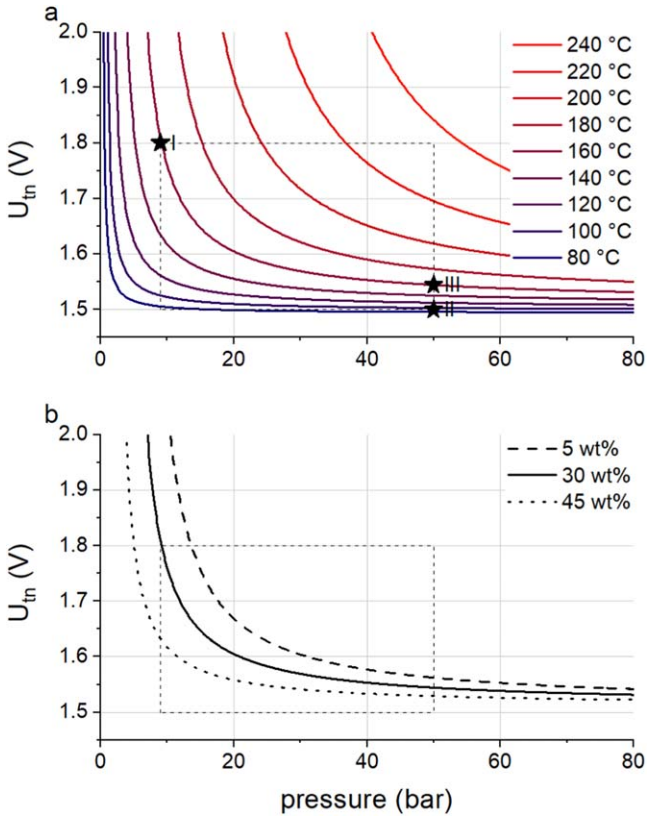

Figure 9. Dependence of the thermoneutral voltage V_{tn} on the operating pressure for 30 wt.% KOH and different temperatures (a) and different KOH concentrations at 160 °C (b), calculated according to Ref. 34 with the vapor pressure according to Ref. 144. The dashed line indicates the minimum and maximum voltage and pressure examples stated in the text.

evaporation per H_2 (Q_{vap}) therefore depends on the water vapor pressure of the electrolyte (p_{vap}) and the operating pressure (p) and can be calculated from the amount of evaporated water per hydrogen gas ($p_{vap}/(p\text{-}p_{vap})$), multiplied with the evaporation enthalpy of water (ΔH_{vap}) and a factor of 1.5 as evaporation takes place on the oxygen side as well, but only 0.5 O_2 are produced per H_2.[34,37,41] Q_{vap} can be expressed as a voltage (U_{vap}) in the same way as the reaction enthalpy (see section on thermodynamics)[34,37,41]:

$$U_{vap} = \frac{Q_{vap}}{2F} = \frac{\Delta H_{vap}}{2F}\frac{1.5p_{vap}}{p - p_{vap}}$$

where F is Faraday's constant. The thermoneutral voltage U_{tn} is the sum of U_{HHV} and U_{vap}. Setting the pressure therefore allows the heat balance of an electrolyzer to be adjusted. Accordingly, for a given overvoltage, electrolyte concentration, and temperature the pressure can be chosen so that no external cooling or heating is necessary, which could offer great simplifications of electrolyzer systems.

Figure 9a shows the pressure-dependence of the thermoneutral voltage for various temperatures with 30 wt.% KOH as the electrolyte. The influence of the temperature is primarily via the change in the vapor pressure of the electrolyte, calculated according to Balej.[144] U_{tn} increases with temperature and decreases with pressure. At high voltages, which occur at relevant high current densities, a high temperature or very low pressure is needed for thermoneutral operation. At low voltages, high pressure or low temperature is necessary. Evidently, the thermoneutral voltage varies with the concentration of KOH, as is depicted in Fig. 9b. Higher concentrations decrease the water vapor pressure and so the thermoneutral voltage.

Figure 9a also illustrates the operating window of an HT-AE electrolyzer: we can assume a voltage limit of 1.8 V to obtain a voltage efficiency of 82%$_{HHV}$ and a reasonable pressure range of 9–50 bar. This yields a minimum temperature of ca 160 °C for thermally-balanced operation at the high voltage/low pressure limit (point I). At a low voltage of 1.51 V, 50 bar is not sufficient for thermoneutral operation at 160 °C and the temperature will drop to ca. 100 °C (point II) if no external heat supply or heat recovery system is employed.[43,145] In order to maintain 160 °C, 1.54 V are necessary at 50 bar (point III). From the figure it can also be seen that thermoneutral operation is a unique possibility for alkaline electrolysis at high temperatures: At 80 °C and 1.8 V, the necessary absolute pressure is below one bar and therefore not practical. At atmospheric pressure, at least 91.5 °C are necessary. Pressure-controlled elecrolyzers usually require a certain minimum pressure, and even a low minimum pressure of two bar results in a minimum temperature of 110 °C. This temperature can thus be considered the minimum for pressure-controlled thermally-balanced operation at this KOH concentration. Above 220 °C, excessively high pressures are required. High pressure increases hydrogen crossover,[118] which presents a safety issue, especially at low current densities. In addition, pressures that are too high can reduce the overall efficiency of hydrogen generation and compression[41,146,147] and increase investment costs.

In practical terms, other heat losses, such as heat dissipation to the surrounding environment and the reheating of condensed water from gas drying, must also be taken into account, yielding the thermal-balance voltage. These depend on the current density, design, isolation, and surface emissivity of the specific electrolyzer[34,143] and can therefore not be estimated based only on thermodynamics. However, the thermal-balance voltage will always be higher than the thermoneutral voltage, and therefore an actual electrolyzer will need to have a slightly increased pressure or reduced temperature compared to an ideal electrolyzer operating at the same voltage.[34,37,43] Heat losses that are independent of the current density, such as the dissipation of heat to the environment, will be especially important at low current densities, i.e., low voltages. Therefore, the difference between the thermoneutral and thermal-balance voltages increases with decreasing current density. These heat losses can be reduced, e.g., by using waste heat from gas cooling and drying to preheat feed water. Kunstreich and Sterlini suggested an energy recovery process to improve the efficiency of electrolysis at high temperatures.[145] Their calculations revealed a significant reduction in the thermal-balance voltage and reduced optimal operating pressures. However, process optimization and scale-up have not received much attention thus far.[138,148] To the best of our knowledge, thermally-balanced operation by pressure control has not yet been experimentally-investigated, even though the idea has been put forward in a patent application,[149] as well as through a publication.[37] The prerequisite of a suitable vapor pressure, which is only present at high temperatures, might be one reason for this.

Thermally-balanced operation by pressure control could enable the simplification of an HT-AE by eliminating heating or cooling devices in the lye circuits. Evidently, the heat stored in the evaporated water must be removed at a later stage, when the product gases are cooled and the water vapor condenses. The gas coolers would therefore need to be larger, but this should be much less demanding than heat exchangers in a viscous and corrosive lye circuit. In addition, the heat transfer in a condenser is generally higher with a low fraction of non-condensing gas.[150] Given the harsh corrosion conditions and the need for special materials, this could represent a significant improvement in terms of investment costs and safety. In addition, simplifying the lye circuits could facilitate the use of natural circulation instead of pumps. First, the pressure drop in the lye circuits should be reduced, accelerating natural circulation. Second, the need for fast circulation to maintain the temperature in the stack is relaxed. One of the main reasons for the typically high flow rates is heat removal, which is eased during thermally-balanced operation when the heat of evaporation is consumed directly in the

Table V. Potential properties and materials for future high-temperature alkaline electrolyzers. PFA: Perfluoroalkoxy alkane, PPS: Polyphenylene sulfide.

Temperature	150 °C–200 °C
Pressure	10–50 bar
Current density	3.75 A cm^{-2} @ <1.8 V
Thermal management	thermally balanced operation
Anode	mixed oxide Ni,Fe or Co
Cathode	Raney-Ni-Mo
Diaphragm	porous zirconia < 100 μm thick
Metal parts	Alloy 400, 800 or passivated Ni
Polymer parts	PTFE, PFA or PPS

stack, where the product gases evolve. Such an HT-AE with thermally-balanced operation and natural convection would have significantly fewer moving parts and costly components, which will reduce both investment costs and maintenance. A detailed evaluation of these advantages requires further research and data on cell performance, material stability, and the feasibility of the outlined simplifications.

Thermally-balanced operation is thus a unique opportunity of electrolysis at high temperature and allows significant simplification of the electrolysis system.

Conclusions

Alkaline electrolysis at high temperature shows great promise to become an efficient, scalable and low-cost method for green hydrogen production. The increased temperature leads to significantly reduced cell voltages, which leads to increased current density and efficiency. Up until now, there has been a lack of comparable data to quantify the improvements, but current densities of 3.75 A cm^{-2} at 1.75 V and 200 °C have already been demonstrated and even better performance should be attainable. Table V summarizes the potential performance and components of an HT alkaline electrolyzer.

Unfortunately, only a few studies in the literature have addressed material stability in the peculiar conditions of HT-AE. Further research is therefore needed to understand the break-away corrosion phenomenon, passivation, and stress corrosion cracking of the different (Ni-) alloys. However, the present data suggests that alloy 400 (67Ni-31.5Cu-1.2Fe) could be suitable for laboratory setups and alloy 800 (33Ni-21Cr-40Fe) or iron-passivated nickel are both promising candidates for long-term stability up to 200 °C. Several other promising alloys still need to be tested. The choice of polymers that can withstand the harsh operating conditions is limited, but at least PTFE and PFA are stable and easily available. If the temperature range is limited, e.g., to 150 °C, the material selection constraints are significantly relaxed.

Stable catalysts for at least up to 160 °C are known; cobalt oxides for the anode, and Mo-or Ti-stabilized Raney nickel for the cathode. Further investigation of their stability and other potentially high-performing stable catalysts such as Ni–Fe–hydroxides under HT-AE conditions is needed, and materials from low-temperature alkaline electrolysis or harsh electrochemical processes such as molten carbonate fuel cells or molten hydroxide electrolysis hold promise. Still, anode stability is probably the biggest challenge for HT-AE.

Stable and thin porous oxide diaphragms made of titanates or zirconia with a thickness down to 180 μm have been demonstrated and further improvements can be expected. Composite diaphragms are also promising, but stable hydrophilicity above 120 °C remains a challenge. Dense anion-conducting composite membranes for high temperature have not yet been explored, but would enable differential pressure operation and lower KOH concentrations.

At the system level, a temperature of at least 110 °C enables efficient thermally-balanced operation at reasonable pressure, which can significantly simplify the electrolyzer. This temperature is well within reach in terms of materials stability. More research is needed to evaluate the feasibility, advantages, disadvantages and optimal temperature of this approach.

Alkaline electrolysis at high temperatures offers unique performance gains and opportunities for all scales from the catalyst to process engineering. The design and operation of an alkaline electrolyzer for high temperatures is certainly challenging, but achievable. Suitable materials are readily available for up to 150 °C, and promising candidates for up to 200 °C are known. More research to improve the components and understanding of this emerging technology is therefore needed, and will also provide the basis for future optimization and techno-economic analysis. If operation at high temperatures is successfully implemented for alkaline water electrolysis, this could also pave the way to advance other important electrochemical processes which suffer from high overpotentials. This includes key processes like CO_2 reduction, ammonia synthesis, and direct fuel cells.

Acknowledgments

The authors would like to thank Vince Bayer (Greenlight Innovation) for discussions on corrosion stability and Hans Hofmann (formerly GHW GmbH) for the exchange regarding high-temperature alkaline electrolysis. Furthermore, we are grateful to Andreas Tschauder, Fabian Scheepers, Edward Rauls, and Michael Hehemann (Forschungszentrum Jülich) for repeated discussions about alloys, thermodynamic limitations, and process design. This work has been supported by the German Federal Ministry of Education and Research, grant no. 03EK3061.

ORCID

F. P. Lohmann-Richters https://orcid.org/0000-0003-3856-9318
S. Renz https://orcid.org/0000-0002-6669-6827

References

1. F. Allebrod, C. Chatzichristodoulou, and M. B. Mogensen, *J. Power Sources*, **229**, 22 (2013).
2. C. Chatzichristodoulou, F. Allebrod, and M. B. Mogensen, *J. Electrochem. Soc.*, **163**, F3036 (2016).
3. J. Divisek, J. Mergel, and H. Schmitz, *Int. J. Hydrogen Energy*, **7**, 695 (1982).
4. J. C. Ganley, *Int. J. Hydrogen Energy*, **34**, 3604 (2009).
5. M. H. Miles, G. Kissel, P. W. T. Lu, and S. Srinivasan, *J. Electrochem. Soc.*, **123**, 332 (1976).
6. H. Wendt, H. Hofmann, H. Berg, V. Plzak, and J. Fischer, *Hydrogen as an energy carrier : Proceedings of the 3rd international seminar, 25.05.83-27.05.83*, Lyon, France25.05.83-27.05.83, ed. G. Imarisio (Reidel)**3**, 267 (1983).
7. J. O. Jensen, C. Chatzichristodoulou, E. Christensen, N. J. Bjerrum, and Q. Li, *in Electrochemical Methods for Hydrogen Production*, 253 (2019).
8. J. Fischer, H. Hofmann, G. Luft, and H. Wendt, *AlChE J.*, **26**, 794 (1980).
9. H. Wendt and G. Imarisio, *J. Appl. Electrochem.*, **18**, 1 (1988).
10. S. D. Ebbesen, S. H. Jensen, A. Hauch, and M. B. Mogensen, *Chem. Rev.*, **114**, 10697 (2014).
11. H. Xu, (2020), DOE H2 Annual Merit Review Meeting: High-Temperature Alkaline Water Electrolysis https://www.hydrogen.energy.gov/annual_review20_h2fuel.html.
12. D. Aili, M. K. Hansen, C. Pan, Q. F. Li, E. Christensen, J. O. Jensen, and N. J. Bjerrum, *Int. J. Hydrogen Energy*, **36**, 6985 (2011).
13. A. V. Nikiforov, I. M. Petrushina, E. Christensen, A. L. Tomas-Garcia, and N. J. Bjerrum, *Int. J. Hydrogen Energy*, **36**, 111 (2011).
14. M. Kouřil, E. Christensen, S. Eriksen, and B. Gillesberg, *Mater. Corros.*, **63**, 310 (2012).
15. J. Mališ, P. Mazúr, M. Paidar, T. Bystron, and K. Bouzek, *Int. J. Hydrogen Energy*, **41**, 2177 (2016).
16. X. Sun, S. C. Simonsen, T. Norby, and A. Chatzitakis, *Membranes*, **9**83 (2019).
17. M. Mandal, *ChemElectroChem*, **8**, 36 (2021).
18. H. A. Miller, K. Bouzek, J. Hnat, S. Loos, C. I. Bernaecker, T. Weissgarber, L. Rontzsch, and J. Meier-Haack, *Sustain. Energy Fuels*, **4**, 2114 (2020).
19. K. F. L. Hagesteijn, S. X. Jiang, and B. P. Ladewig, *J. Mater. Sci.*, **53**, 11131 (2018).
20. N. Chen and Y. M. Lee, *Prog. Polym. Sci.*, **113**101345 (2021).
21. W. E. Mustain, M. Chatenet, M. Page, and Y. S. Kim, *Energy Environ. Sci.*, **13**, 2805 (2020).
22. A. Goñi-Urtiaga, D. Presvytes, and K. Scott, *Int. J. Hydrogen Energy*, **37**, 3358 (2012).

23. S. Meyer, A. V. Nikiforov, I. M. Petrushina, K. Kohler, E. Christensen, J. O. Jensen, and N. J. Bjerrum, *Int. J. Hydrogen Energy*, **40**, 2905 (2015).
24. N. Fujiwara, H. Nagase, S. Tada, and R. Kikuchi, *ChemSusChem*, **14**, 417 (2021).
25. H. Vandenborre, R. Leysen, H. Nackaerts, and P. Van Asbroeck, *Hydrogen energy progress IV; proceedings of the 4th World Hydrogen Energy Conference, 13.6. – 17.6.1982*, ed. T. N. Veziroglu (Pergamon, Pasadena, California) 1, 107 (1982).
26. I. Abe, T. Fujimaki, and M. Matsubara, *Int. J. Hydrogen Energy*, **9**, 753 (1984).
27. R. A. Brand and H. Hofmann, *10. Symposium Nutzung Regenerativer Energiequellen und Wasserstofftechnik*, ed. J. Lehmann and W. Beckmann (Fachhochschule Stralsund, Germany, Stralsund)11 (2003).
28. C. A. Schug, *Int. J. Hydrogen Energy*, **23**, 1113 (1998).
29. M. David, C. Ocampo-Martinez, and R. Sanchez-Pena, *Journal of Energy Storage*, **23**, 392 (2019).
30. J. Brauns and T. Turek, *Processes*, **8**, 248 (2020).
31. F. Allebrod, C. Chatzichristodoulou, and M. B. Mogensen, *J. Power Sources*, **255**, 394 (2014).
32. A. Buttler and H. Spliethoff, *Renew. Sust. Energ. Rev.,*, **82**, 2440 (2018).
33. J. Balej, *Int. J. Hydrogen Energy*, **10**, 365 (1985).
34. R. L. Leroy, C. T. Bowen, and D. J. Leroy, *J. Electrochem. Soc.*, **127**, 1954 (1980).
35. S. K. Mazloomi and N. Sulaiman, *Renew. Sust. Energ. Rev.*, **16**, 4257 (2012).
36. P. Millet, *Hydrogen Production: by Electrolysis*, ed. A. Godula-Jopek (Wiley, Weinheim)33 (2015).
37. Y. Ogata, M. Yasuda, and F. Hine, *J. Electrochem. Soc.*, **135**, 2976 (1988).
38. NIST-JANAF, *Thermochemical Tables* (American Institute of Physics, Washington, DC: New York) (1998).
39. I. Abe, T. Fujimaki, and M. Matsubara, *Hydrogen energy progress IV; proceedings of the 4th World Hydrogen Energy Conference, 13.6. – 17.6.1982*, ed. T. N. Veziroglu (Pergamon, Pasadena, California) 1, 167 (1982).
40. M. Suermann, T. J. Schmidt, and F. N. Buchi, *Electrochim. Acta*, **211**, 989 (2016).
41. F. Scheepers, M. Stähler, A. Stähler, E. Rauls, M. Müller, M. Carmo, and W. Lehnert, *Energies*, **13**, 612 (2020).
42. H. Wendt, H. Hofmann, and V. Plzak, *Int. J. Hydrogen Energy*, **9**, 297 (1984).
43. R. L. Leroy, *J. Electrochem. Soc.*, **130**, 2158 (1983).
44. M. Prigent, T. Nenner, L. Martin, and M. Roux, *Hydrogen As An Energy Carrier: Proceedings of the 3rd international seminar*, Lyon, France 25.05.83-27.05.83, ed. G. Imarisio (Reidel)**3**, 256-266 (1983).
45. H. Wendt and V. Plzak, *Electrochim. Acta*, **28**, 27 (1983).
46. Y. Ogata, H. Hori, M. Yasuda, and F. Hine, *J. Electrochem. Soc.*, **135**, 76 (1988).
47. C. R. Davidson, G. Kissel, and S. Srinivasan, *J. Electroanal. Chem.*, **132**, 129 (1982).
48. F. Allebrod, "High Temperature and Pressure Alkaline Electrolysis." *PhD Thesis*, Department of energy conversion and storage, Technical University of Denmark (2013).
49. J. Balej, *Int. J. Hydrogen Energy*, **10**, 89 (1985).
50. F. Allebrod, C. Chatzichristodoulou, P. L. Mollerup, and M. B. Mogensen, *Int. J. Hydrogen Energy*, **37**, 16505 (2012).
51. R. J. Gilliam, J. W. Graydon, D. W. Kirk, and S. J. Thorpe, *Int. J. Hydrogen Energy*, **32**, 359 (2007).
52. D. A. Lown and H. R. Thirsk, *Trans. Faraday Soc.*, **67**, 132 (1971).
53. W. M. Vogel, K. Routsis, V. J. Kehrer Jr, D. A. Landsman, and J. G. Tschinkel, *J. Chem. Eng. Data*, **12**, 465 (1967).
54. V. Y. Yushkevich, I. Maksimova, and V. Bullan, *Elektrokhimiya*, **3**, 1491 (1967).
55. D. M. See and R. E. White, *J. Chem. Eng. Data*, **42**, 1266 (1997).
56. J. R. Crum, *Corrosion*, **42**, 368 (1986).
57. J. R. Crum and L. E. Shoemaker, *NACE*, **06219** (2006).
58. R. S. Pathania and R. D. Cleland, *Corrosion*, **41**, 575 (1985).
59. G. Kreysa and M. Schuetze, *Corrosion Handbook: Potassium Hydroxide, ammonium and Ammonium Hydroxide* (Wiley, Weinheim) (2007).
60. F. W. Pement, I. L. W. Wilson, and R. G. Aspden, *Mater. Performance*, **19**, 43 (1980).
61. W. Yang, Z. P. Lu, D. L. Huang, D. S. Kong, G. Z. Zhao, and J. Congleton, *Corros. Sci.*, **43**, 963 (2001).
62. INCO International Nickel Company Inc., (1973, 2020), Corrosion Resistance of Nickel and Nickel-Containing Alloys in Caustic Soda and other Alkalies (CEB-2), Nickel Institute https://nickelinstitute.org/media/4685/ni_inco_281_corrosionresistcausticalkalies.pdf.
63. I. Abe, T. Fujimaki, Y. Kajiwara, and Y. Yokoo, *Hydrogen Energy Progress. 3,1: Proceedings of the 3rd World Hydrogen Energy Conference, 23.6. – 26.6.80*, ed. T. N. Veziroglu (Pergamon, Tokyo) 1, 29 (1980).
64. P. Combrade, *Rapport Final EUR 10033 FR: Étude de la résistance à la corrosion du nickel et d'alliages à base de nickel dans les électrolyseurs d'eau travaillant à 200 degrés C* (Commission of the European Communities, Luxembourg) (1985).
65. J. M. Gras and P. Spiteri, *Int. J. Hydrogen Energy*, **18**, 561 (1993).
66. H. Wendt and H. Hofmann, *Hydrogen as an energy carrier: Proceedings of the 3rd international seminar,* , Lyon, France25.05.83-27.05.83, ed. G. Imarisio (Reidel)**3**, 286 (1983) .
67. H. Wendt and H. Hofmann, *Int. J. Hydrogen Energy*, **10**, 375 (1985).
68. A. Garat and J. M. Gras, *Int. J. Hydrogen Energy*, **8**, 681 (1983).
69. T. Rauscher, C. I. Bernacker, U. Muhle, B. Kieback, and L. Rontzsch, *Int. J. Hydrogen Energy*, **44**, 6392 (2019).
70. Z. Wu, Z. Zou, J. Huang, and F. Gao, *ACS Appl. Mater. Interfaces*, **10**, 26283 (2018).
71. Y. Wu, M. J. Zhao, F. Li, J. Xie, Y. Li, and J. B. He, *Langmuir*, **36**, 5126 (2020).
72. R. L. Leroy, *Int. J. Hydrogen Energy*, **8**, 401 (1983).
73. R. B. Rebak, *Stress Corrosion Cracking*, ed. V. S. Raja and T. Shoji (Woodhead Publishing)273 (2011).
74. K. M. Pruett, *Chemical Resistance Guide For Metals And Alloys Ii: A Guide To Chemical Resistance Of Metals And Alloys* (Compass Publications, La Jolla, CA) (2012).
75. A. Mignone, M. F. Maday, A. Borello, and M. Vittori, *Corrosion*, **46**, 57 (1990).
76. J. Kwon, H. Han, S. Choi, K. Park, S. Jo, U. Paik, and T. Song, *ChemCatChem*, **11**, 5898 (2019).
77. H. Jin, B. Ruqia, Y. Park, H. J. Kim, H. S. Oh, S. I. Choi, and K. Lee, *Adv. Energy Mater.*, **11**, 2003188 (2021).
78. D. J. Zhou, P. S. Li, W. W. Xu, S. Jawaid, J. Mohammed-Ibrahim, W. Liu, Y. Kuang, and X. M. Sun, *Chemnanomat*, **6**, 336 (2020).
79. C. Hu, L. Zhang, and J. Gong, *Energy Environ. Sci.*, **12**, 2620 (2019).
80. N. K. Chaudhari, H. Jin, B. Kim, and K. Lee, *Nanoscale*, **9**, 12231 (2017).
81. J. Divisek and H. Schmitz, *Int. J. Hydrogen Energy*, **7**, 703 (1982).
82. C. Liu et al., *Adv. Energy Mater.*, **11**, 2002926 (2021).
83. C. Rakousky, U. Reimer, K. Wippermann, M. Carmo, W. Lueke, and D. Stolten, *J. Power Sources*, **326**, 120 (2016).
84. J. Divisek, P. Malinowski, J. Mergel, and H. Schmitz, *Int. J. Hydrogen Energy*, **13**, 141 (1988).
85. M. Prigent and T. Nenner, *Hydrogen Energy Progress IV; Proceedings of the 4th World Hydrogen Energy Conference, 13.6. – 17.6.1982'*, ed. T. N. Veziroglu (Pergamon, Oxford: Pasadena, California) 1, 299 (1982).
86. R. D. Giles, *Hydrogen Energy Progress IV; Proceedings of the 4th World Hydrogen Energy Conference*, ed. T. N. Veziroglu (Pergamon, Pasadena, California) 1, 279 (1982).
87. H. Wendt, H. Hofmann, and V. Plzak, *Mater. Chem. Phys.*, **22**, 27 (1989).
88. H. Vandenborre, R. Leysen, H. Nackaerts, P. Van Asbroeck, and J. Piepers, *Hydrogen As An Energy Carrier: Proceedings of the 3rd International Seminar*, Lyon, France25.05.83-27.05.83, ed. G. Imarisio (Reidel)**3**, 139 (1983).
89. J. Q. Adolphsen, B. R. Sudireddy, V. Gil, and C. Chatzichristodoulou, *J. Electrochem. Soc.*, **165**, F827 (2018).
90. T. Schmidt and H. Wendt, *Electrochim. Acta*, **39**, 1763 (1994).
91. F. Hine, M. Yasuda, and M. Watanabe, *Denki Kagaku oyobi Kogyo Butsuri Kagaku*, **47**, 401 (1979).
92. M. Christy, H. Rajan, H. Yang, and Y.-B. Kim, *Energy & Fuels*, **34**, 16838 (2020).
93. D. D. Matienzo, T. Kutlusoy, S. Divanis, C. Di Bari, and E. Instuli, *Catalysts*, **10**, 1387 (2020).
94. A. Kulkarni and S. Giddey, *J. Solid State Electrochem.*, **16**, 3123 (2012).
95. S. Anantharaj, S. Noda, V. R. Jothi, S. Yi, M. Driess, and P. W. Menezes, *Angew. Chem. Int. Ed. Engl.*, **60**, 18981 (2021).
96. K. Zeng and D. Zhang, *Prog. Energy Combust. Sci.*, **36**, 307 (2010).
97. M. Schalenbach, O. Kasian, and K. J. J. Mayrhofer, *Int. J. Hydrogen Energy*, **43**, 11932 (2018).
98. G. Schiller, R. Henne, P. Mohr, and V. Peinecke, *Int. J. Hydrogen Energy*, **23**, 761 (1998).
99. L. Wang, T. Weissbach, R. Reissner, A. Ansar, A. S. Gago, S. Holdcroft, and K. A. Friedrich, *ACS Appl. Energy Mater.*, **2**, 7903 (2019).
100. S. H. Kim, Y. S. Park, C. Kim, I. Y. Kwon, J. Lee, H. Jin, Y. S. Lee, S. M. Choi, and Y. Kim, *Energy Reports*, **6**, 248 (2020).
101. P. M. Bodhankar, P. B. Sarawade, G. Singh, A. Vinu, and D. S. Dhawale, *J. Mater. Chem. A*, **9**, 3180 (2021).
102. L. Yang, Z. Liu, S. Zhu, L. Feng, and W. Xing, *Mater. Today Phys.*, **16**, 100292 (2021).
103. A. Karmakar, K. Karthick, S. S. Sankar, S. Kumaravel, R. Madhu, and S. Kundu, *J. Mater. Chem. A*, **9**, 1314 (2021).
104. Z. Qiu, C.-W. Tai, G. A. Niklasson, and T. Edvinsson, *Energy Environ. Sci.*, **12**, 572 (2019).
105. S. Anantharaj, S. Kundu, and S. Noda, *Nano Energy*, **80**, 105514 (2021).
106. X. Xie, C. Cao, W. Wei, S. Zhou, X. T. Wu, and Q. L. Zhu, *Nanoscale*, **12**, 5817 (2020).
107. M. Su, S. Zhu, Z. Cui, Z. Li, S. Wu, M. Guo, H. Jiang, and Y. Liang, *Sustain. Energy Fuels*, **5**, 3205 (2021).
108. X. Liu, M. Gong, S. Deng, T. Zhao, T. Shen, J. Zhang, and D. Wang, *Adv. Funct. Mater.*, **31**, 2009032 (2020).
109. J. Li and J. Gong, *Energy Environ. Sci.*, **13**, 3748 (2020).
110. X. X. Zheng, A. J. Bottger, K. M. B. Jansen, J. van Turnhout, and J. van Kranendonk, *Front. Mater.*, **7**, 437 (2020).
111. D. Aili, K. Jankova, Q. F. Li, N. J. Bjerrum, and J. O. Jensen, *J. Membr. Sci.*, **492**, 422 (2015).
112. R. Renaud and R. Leroy, *Int. J. Hydrogen Energy*, **7**, 155 (1982).
113. P. Millet and N. Guillet, *Hydrogen Production: by Electrolysis*, ed. A. Godula-Jopek (Wiley, Weinheim)117 (2015).
114. P. H. Vermeiren, R. Leysen, H. Beckers, J. P. Moreels, and A. Claes, *J. Porous Mater.*, **15**, 259 (2006).
115. N. V. Agfa-Gevaert, (2020), Technical Data Sheet ZIRFON PERL UTP 500 https://www.agfa.com/specialty-products/solutions/membranes/zirfon/.
116. M. Schalenbach, A. R. Zeradjanin, O. Kasian, S. Cherevko, and K. J. J. Mayrhofer, *Int. J. Electrochem. Sci.*, **13**, 1173 (2018).
117. H. Wendt and H. Hofmann, *J. Appl. Electrochem.*, **19**, 605 (1989).
118. M. Schalenbach, W. Lueke, and D. Stolten, *J. Electrochem. Soc.*, **163**, F1480 (2016).
119. P. Haug, M. Koj, and T. Turek, *Int. J. Hydrogen Energy*, **42**, 9406 (2017).
120. P. Trinke, P. Haug, J. Brauns, B. Bensmann, R. Hanke-Rauschenbach, and T. Turek, *J. Electrochem. Soc.*, **165**, F502 (2018).
121. J. Divisek, P. Malinowski, J. Mergel, and H. Schmitz, *Int. J. Hydrogen Energy*, **10**, 383 (1985).
122. T. Nenner and A. Fahrasmane, *Int. J. Hydrogen Energy*, **9**, 309 (1984).

123. J. C. Sohm and L. Mas, *Hydrogen as an Energy Vector*, ed. A. A. Strub and G. Imarisio (Springer, Netherlands, Dordrecht)323 (1980).
124. H. Vandenborre, R. Leysen, T. Nenner, and M. Roux, *Hydrogen as an energy carrier: Proceedings of the 3rd international seminar, 25.05.83-27.05.83*, ed. G. Imarisio (Reidel, Dordrecht: Lyon) 3, 305 (1983).
125. R. Dick and P. Faye, *Hydrogen As An Energy Carrier: Proceedings of the 3rd International Seminar, 25.05.83-27.05.83*, ed. G. Imarisio (Reidel, Lyon) 3, 330 (1983).
126. H. S. Kim, Y. Yamazaki, J. D. Kim, T. Kudo, and I. Honma, *Solid State Ion.*, **181**, 883 (2010).
127. F. P. Lohmann-Richters, M. Mueller, and M. Carmo, *J. Electrochem. Soc.*, **167**, 084512 (2020).
128. R. K. Nishihora, P. L. Rachadel, M. G. N. Quadri, and D. Hotza, *J. Eur. Ceram. Soc.*, **38**, 988 (2018).
129. O. Guillon, A. Dash, C. Lenser, S. Uhlenbruck, and G. Mauer, *Adv. Eng. Mater.*, **22**, 2000529 (2020).
130. N. Hedayat, Y. Du, and H. Ilkhani, *Renew. Sust. Energ. Rev.*, **77**, 1221 (2017).
131. L. J. Bonderer, P. W. Chen, P. Kocher, and L. J. Gauckler, *J. Am. Ceram. Soc.*, **93**, 3624 (2010).
132. H. Qin, W. M. Guo, X. Huang, P. Z. Gao, and H. N. Xiao, *J. Eur. Ceram. Soc.*, **40**, 145 (2020).
133. M. Tanahashi, *Materials*, **3**, 1593 (2010).
134. N. V. Agfa-Gevaert, (2020), Technical Data Sheet ZIRFON UTP 500+ https://www.agfa.com/specialty-products/solutions/membranes/zirfon/.
135. M. Schalenbach, G. Tjarks, M. Carmo, W. Lueke, M. Mueller, and D. Stolten, *J. Electrochem. Soc.*, **163**, F3197 (2016).
136. H. In Lee, D. T. Dung, J. Kim, J. H. Pak, S. k. Kim, H. S. Cho, W. C. Cho, and C. H. Kim, *Int. J. Energy Res.*, **44**, 1875 (2019).
137. M. Bonanno, K. Müller, B. Bensmann, R. Hanke-Rauschenbach, R. Peach, and S. Thiele, *J. Electrochem. Soc.*, **168**, 094504 (2021).
138. S. Dutta, *Int. J. Hydrogen Energy*, **15**, 379 (1990).
139. B. V. Tilak, P. W. T. Lu, J. E. Colman, and S. Srinivasan, *Comprehensive Treatise of Electrochemistry*, ed. J. O. M. Bockris, B. E. Conway, E. Yeager, and R. E. White (Springer, Berlin: US, Boston, MA)1 (1981).
140. S. A. Grigoriev, V. N. Fateev, D. G. Bessarabov, and P. Millet, *Int. J. Hydrogen Energy*, **45**, 26036 (2020).
141. H. Li, A. Inada, T. Fujigaya, H. Nakajima, K. Sasaki, and K. Ito, *J. Power Sources*, **318**, 192 (2016).
142. J. M. Spurgeon and N. S. Lewis, *Energy Environ. Sci.*, **4**, 2993 (2011).
143. Y. Ogata, S. Kainuma, M. Yasuda, and F. Hine, *J. Electrochem. Soc.*, **132**, 2594 (1985).
144. J. Balej, *Int. J. Hydrogen Energy*, **10**, 233 (1985).
145. S. Kunstreich and J. Sterlini, *Hydrogen energy system; Proceedings of the Second World Hydrogen Energy Conference, Zurich, Switzerland, August 21-24, 1978.*, ed. T. N. Veziroglu and W. Seifritz (Pergamon, New York, NY) 5, 2413 (1979).
146. G. Tjarks, A. Gibelhaus, F. Lanzerath, M. Müller, A. Bardow, and D. Stolten, *Appl. Energy*, **218**, 192 (2018).
147. F. Scheepers, M. Stähler, A. Stähler, E. Rauls, M. Müller, M. Carmo, and W. Lehnert, *Appl. Energy,*, **283** (2021).
148. J. Fischer and G. Luft, *Chem. Ing. Tech.*, **57**, 614 (1985).
149. S. Kunstreich, "Process and device for regulating the operation of an electrolytic apparatus used for gas production." *Patent*, EP0004799B1 (1979).
150. W. Roetzel and B. Spang, "*Typical Values of Overall Heat Transfer Coefficients*." *VDI Heat Atlas* (Springer, Berlin, Heidelberg)C3, 75 (2010).